

NONLINEAR HIGH FIDELITY STATIC AEROELASTIC EFFECT ON THE FLEXIBLE PITCHING MOMENT AERODYNAMIC COEFFICIENT FOR A TRANSPORT AIRCRAFT

Angelo A. Verri^{1,2}, Kelvin C. de Moraes¹, Flávio Luiz S. Bussamra² and
Carlos E. S. Cesnik³

¹ EMBRAER S/A – Brazilian Aeronautic Company
São José dos Campos, São Paulo BRAZIL
angelo.verri@embraer.com.br
kelvin.morais@embraer.com.br

² ITA – Technological Institute of Aeronautics
São José dos Campos, São Paulo BRAZIL
flaviobu@ita.br

³ UniMich - University of Michigan
Ann Arbor, Michigan USA
cesnik@umich.edu

Keywords: static loads, static aeroelasticity, fluid-structure interaction, pitching moment coefficient, nonlinear structure.

Abstract: This paper presents a static iterative aero-structural method applied as a study case to a transport aircraft with wing aspect ratio of 12. It evaluates the structure geometric nonlinearity effect on aerodynamic coefficients. A Nonlinear High-fidelity Static Fluid-structure Iteration tool (E2-FSI) was used in this study case. It combines Reynolds Average Navier Stokes Computational Fluid Dynamics with detailed Finite Elements Method in linear and nonlinear structural analyses. The wing body nonlinear high fidelity static aeroelastic effect on flexible pitching moment coefficient was correlated to rigid tail trimming demand showing static tail loads being modified by wing nonlinear flexibility.

1 INTRODUCTION

The aeronautical engineering problems are continuously demanding more efficient solutions. As the wings of transport aircrafts are becoming more flexible [1,2], there is an increase in the application of high fidelity aero-structural analyses. The high fidelity in aerodynamics enables considerable high angles of attack with a consistent formulation and the detailed structure enables local understanding of the design considering the correct flexibility.

Fluid Structure Interaction (FSI), when using high fidelity tools and working with different strategies [3,4,5,6,7], was proven to be well related to wind tunnel tests. For Static Loads technology, there was structure nonlinearity effect on the internal loads along the span of a recent conventional aircraft wing [8], captured by using high fidelity static aeroelastic analyses. The increase on bending moment was small in the wing root. However there was an increase of 11.5% in the outboard portion of the wing.

This paper is a sequence of the above-mentioned study which quantifies the high flexibility aspects of recent aircrafts in order to foresee future methods for upcoming high flexibility aircrafts. The same static aeroelastic method was applied as a study case to a conventional transport aircraft with the aspect ratio of 12. In this case showing a different way to understand the high fidelity static aeroelastic additional output results. It focuses on pitching moment aerodynamic coefficient of the aircraft being modified by the nonlinear structure. The consequence of a different wing-body pitching moment coefficient is a different demand for tail compensation, thus affecting tail static loads.

This study shows the wing nonlinear structure effect on the pitching moment aerodynamic coefficient using static aeroelasticity with high fidelity tools in both aerodynamics and structures. The maximum angle of attack was equivalent to 2.5g ($g=9.8\text{m/s}^2$) static pull-up maneuvers, and the tail rigid reactions were calculated for every stabilized maneuver.

2 E2-FSI

The tool E2-FSI, Nonlinear High-fidelity Static Fluid-structure Iteration, was developed for high flexibility static aeroelastic evaluations at Embraer [9]. Details of the tool are available in former publications [8,10].

The E2-FSI integrates software CFD++ [11] and Nastran® [12] in an iterative process, thus translating aerodynamic results into structural loads and transforming structural results into aerodynamic mesh updates. See Figure 1. An additional block for tail rigid trimming calculation is added at the end of each converged result. The pitching moment for wing-body, using linear or nonlinear structural analyses, is compensated by a rigid trim force in the tail in order to balance the aircraft.

The tail trim was considered rigid, in order to demonstrate the concept. A constant distance for tail trim force was considered.

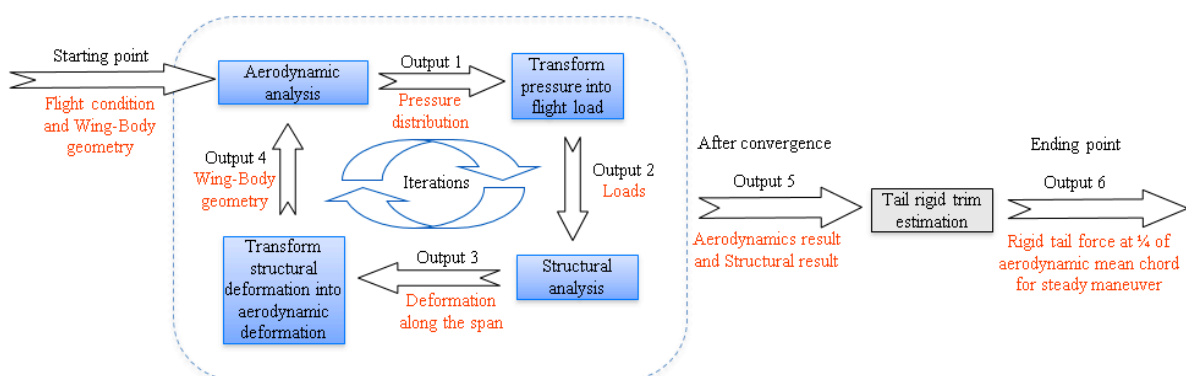


Figure 1 – E2-FSI scheme with additional block for tail rigid trim estimation.

3 AIRCRAFT

Figure 2 shows the conventional transport aircraft used for this investigation. The aircraft has wing aspect ratio of 12 and dimensions of a regional transport aircraft.

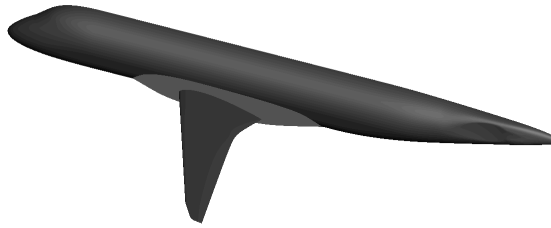


Figure 2 – Wing-body for a transport aircraft model.

4 CFD++

Computational fluid dynamics analysis in CFD++ [11] considered wing-body geometry. Figure 3 shows the aerodynamic mesh in which the fuselage, wing and field symmetry plane meshes are presented. It uses Reynolds Average Navier Stokes Computational Fluid Dynamics (RANS - CFD) so that high angles of attack are evaluated. The turbulence model was Spalart-Allmaras [13]. The solve to wall formulation was used. The wing surface mesh is deformable. The pressure distribution was post-processed to transform it into follower structural loads, which take the wing deformed shape into account.

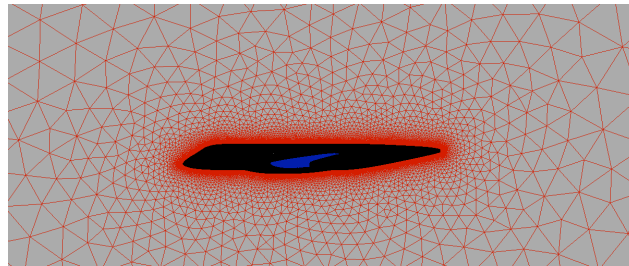


Figure 3 - Wing-Body mesh, side view.

5 NASTRAN®

The left side wing Finite Elements Method (FEM) model is presented in Figure 4. It was clamped in the attachment to the fuselage as a simplification. The detailed structural model was composed by plates and bars. The inertial loads were not considered for this study in order to quantify only the aerodynamic effect. The built-in solver Nastran® was used [14,15]. When the FSI uses static linear structural analysis, it is called E2-FSI Standard. In case FSI uses static geometric nonlinear analysis [16], it is called E2-FSI Featured.

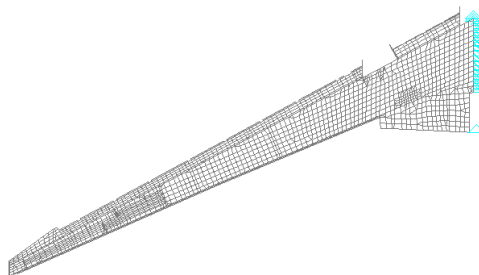


Figure 4 – Wing clamped at the root.

6 RESULTS

Mach 0.70 for 5 different load factors (NZ) are presented in Figure 5 as a result of the E2-FSI Standard. The airfoil rotation at the tip of the wing was plotted for every iteration. The tip airfoil rotation was more negative with the increase in load factor, which means the leading edge going downwards and trailing edge going upwards.

Figure 6 shows the wing-body pitching moment coefficient (CMWB) along the iterations for both the E2-FSI Standard and Featured. At iteration 14 there was a negligible effect of geometric nonlinearity inside the FSI but at iteration 31 the effect is visible. In both cases, there was an increase in CMWB with the increase in load factor. The difference between the Featured and the Standard above 1.5g was a consequence of a different airfoil rotation along the span.

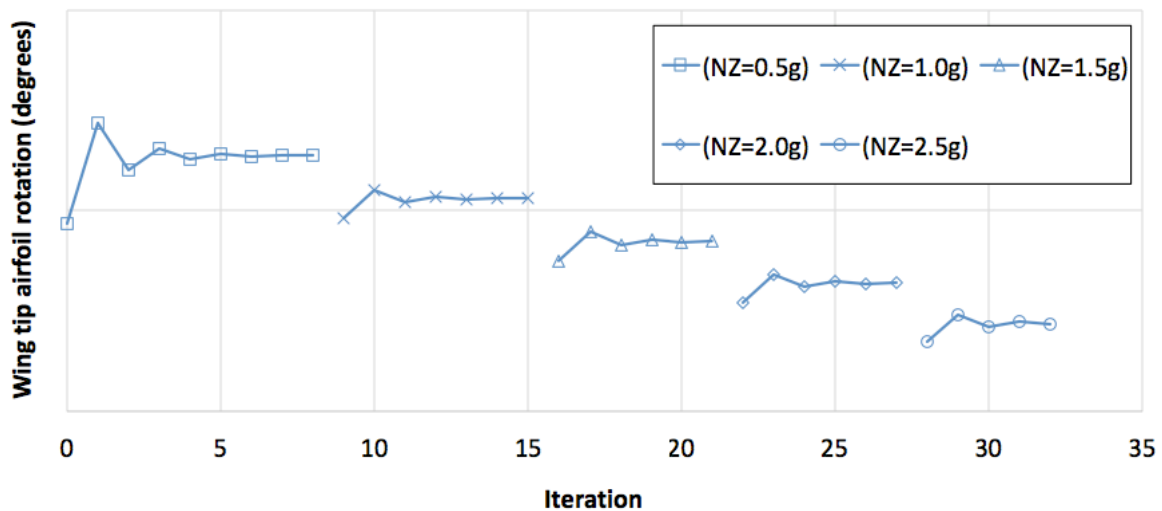


Figure 5 – Airfoil rotation for each iteration.

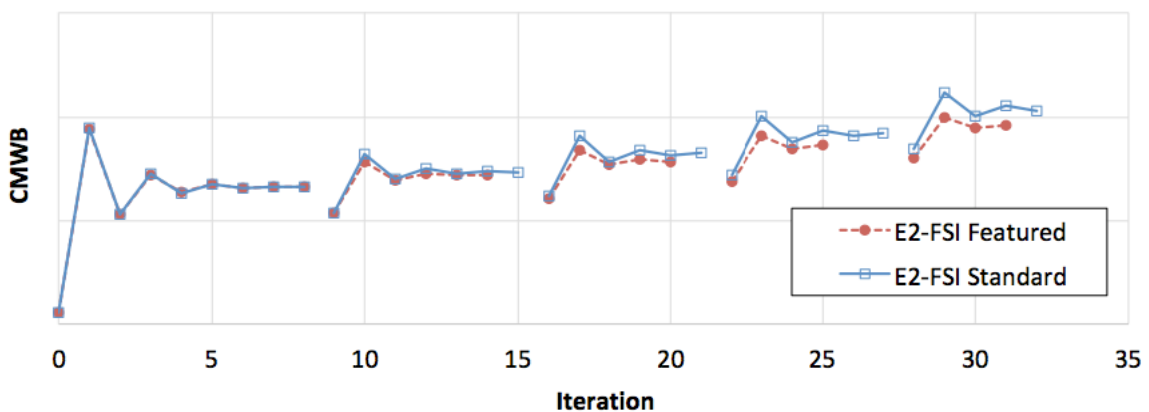


Figure 6 –Pitching moment coefficient along iterations.

Figure 7 presents only the converged results. The plot is for CMWB along angle of attack. Note the increasing difference in the E2-FSI Featured while the angle of attack increases. Around 1.5 degrees, where the load factor is 2.0g, there was a difference of 3.9% in CMWB and 4.5% in the aircraft angle of attack. The main effect was the change in the derivate of CMWB with angle of attack, as expected for flexibility effects. Second order polynomial

trend lines almost match the results. The difference between the Featured and the Standard was in the linear part of the polynomial equation indicating a feasible linear correction for the complex effect.

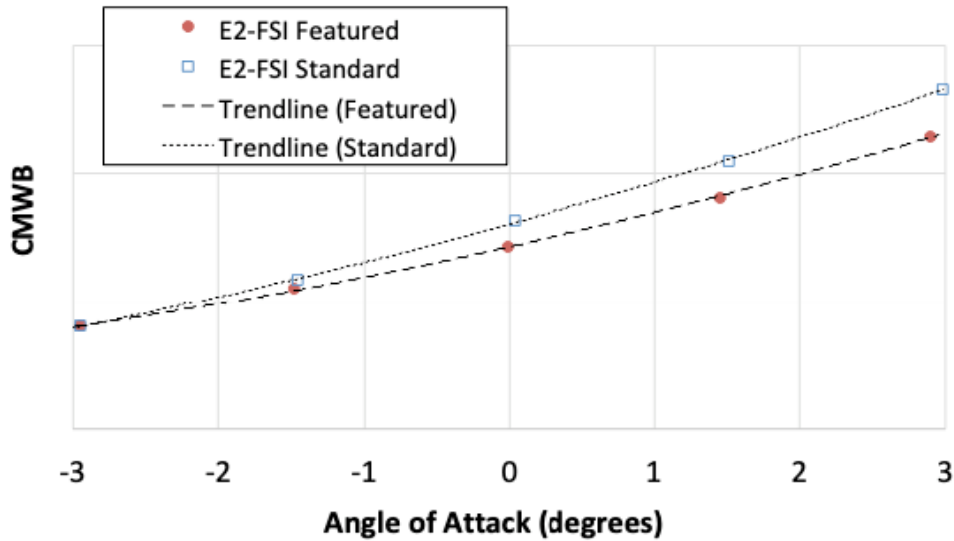


Figure 7 – E2-FSI converged pitching moment with second order trend lines

The difference in CMWB was converted to the necessary vertical force on the horizontal tail in order to trim the aircraft in the maneuver. Figure 8 shows the increase on the horizontal tail vertical force due to the pitching moment high flexibility parcel for wing-body. The difference starts in zero and reaches 5% at 2.5g limit static maneuver. The downwards force in the horizontal tail needs to be 5% bigger in order to trim the aircraft limit maneuver with high flexibility effects. There was no significant influence on the load factor (0.01g reduction on limit maneuver) due to the increase in the tail force, because the wing body lift is much bigger than the tail trim increase. Therefore, the hypothesis of a constant trim for wing-body lift setup was satisfactory.

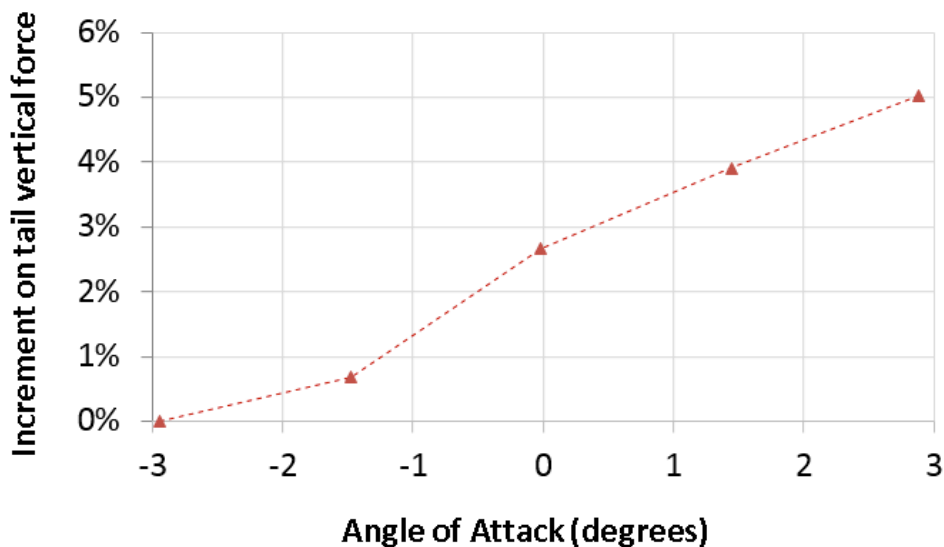


Figure 8 – Tail trim force increment due to structure nonlinearity.

7 CONCLUSIONS

The E2-FSI was used in order to better represent the flight static maneuvers of a flexible aircraft structure with wing aspect ratio 12. The high flexibility effects were quantified for a transport aircraft so future static aeroelastic effect processes can be improved based on the findings of this study case.

The results presented herein have shown effects on pitching moment aerodynamic coefficient due to high flexibility on a transport aircraft. The complex effect on pitching moment versus angle of attack, captured with static aeroelastic nonlinear high fidelity tool, can be represented by a linear derivate correction for the parcel of data analyzed.

There was an increase in tail trim forces during static pull-up maneuvers when the wing high flexibility effect was enabled. There was an increment of 5% at limit static maneuver. Considering the tail loads envelope composed by static and dynamic condition, there was no indication of structural issues for recent aircrafts. As wing flexibility and aspect ratio increase, there is a tendency for more nonlinear effect. Thus, future aircrafts may necessarily consider the presented effect.

8 REFERENCES

- [1] Bradley, M. K., Droney, C. K. (2011). Subsonic Ultra Green Aircraft Research: Phase I Final Report. *Boeing Research & Technology - NASA/CR-2011-216847*.
- [2] Afonso, F., Vale, J., Oliveira, E., Lau, F., Suleman, A. (2017). A review on non-linear aeroelasticity of high aspect-ratio wings. *Progress in Aerospace Sciences, Vol. 89, pages 40-57*.
- [3] Bartels, Robert E., Scott Robert C., Allen, Timothy J., Sexton, Bradley W. (2015). Aeroelastic Analysis of SUGAR Truss-Braced Wing Wind-Tunnel Model Using FUN3D and a Nonlinear Structural Model. *s.l.: 56th AIAA*.
- [4] Bartels, R. E., Scott, R. C., Funk, C. J., Allen, T. J., and Sexton, B. W. (2014). Computed and Experimental Flutter/LCO Onset for the Boeing Truss-Braced Wing Wind-Tunnel Model. *32st AIAA*.
- [5] Eberhardt, S., Benedict, K., Hedges, L., Robinson, A., Tinoco, E. N. (2014). Inclusion of Aeroelastic Twist into the CFD Analysis of the Twin-Engine NASA Common Research Model. *AIAA SciTech*.
- [6] Keye, S., Rudnik, R. (2015). Validation of Wing Deformation Simulations for the NASA CRM Model using Fluid-Structure Interaction Computations. *53rd AIAA Aerospace Sciences Meeting, AIAA SciTech Forum*.
- [7] NASA. 6th AIAA CFD Drag Prediction Workshop. Available at: <https://aiaa-dpw.larc.nasa.gov>. Published on 2016. Accessed on: 03/June/2017.
- [8] Verri, A. A., Morais, K. C., Bussamra, F. L. S., Becker, G. G., Cesnik, C. E. S. (2018). Static Loads Evaluation in a Flexible Aircraft Using High Fidelity Fluid-structure Iteration Tool (E2-FSI). *ICAS 2018*.
- [9] EMBRAER S/A. Official Embraer website. Available at: <https://embraer.com>. Accessed on: 07/June/2018 at 16:00h.
- [10] Verri, A. A., Jorge, C. T., Bizarro, A. F., Bussamra, F. L. S., Júnior, H. N. S., Cesnik, C. E. S. (2018). Multidisciplinary Methods for Wing Flight Shape Analysis – Effect of the Geometric Nonlinear Structure for Static Pull-up. *ICAS 2018*.

- [11] Metacomp. Metacomp Technologies. *Available at: < <http://www.metacomptech.com/>>. Accessed on: 24/May/2018 at 13:00h.*
- [12] MSC. Official website for MSC Nastran software version 2016R1. *Available at: <<http://www.msc software.com/product/msc-nastran>>. Accessed on: 18/Jan/2017 at 7:00h.*
- [13] Spalart, P. R., Allmaras, S. R. (1994). A One-Equation Turbulence Model for Aerodynamic Flows. *Recherche Aerospatiale. 1994*
- [14] MSC (2016). MSC Nastran Nonlinear User's Guide 2016.
- [15] MSC (2012). Nonlinear Structural Analysis with SimXpert. SMX400 Course Notes 2012.
- [16] Bauchau, O. A. and Hong, C. H. (1988). Nonlinear Composite Beam Theory. *Journal of Applied Mechanics - Transactions of the ASME, Vol. 55, No. 1, pp. 156-163.*

COPYRIGHT STATEMENT

The authors confirm that they, and/or their company or organization, hold copyright on all of the original material included in this paper. The authors also confirm that they have obtained permission, from the copyright holder of any third party material included in this paper, to publish it as part of their paper. The authors confirm that they give permission, or have obtained permission from the copyright holder of this paper, for the publication and distribution of this paper as part of the IFASD-2019 proceedings or as individual off-prints from the proceedings.